Acta Universitatis Sapientiae
Electrical and Mechanical Engineering, 16 (2024) 16–25

DOI: 10.47745/auseme-2024-0002

Effect of Blade Number of an Anchor Agitator on the Laminar Flow in a Cylindrical Vessel

Abdelghani BELHANAFI[1], Omar LADJEDEL[1], Lahouari ADJLLOUT[1]

[1] Department of Mechanical Engineering, Faculty of Mechanics,
University of Sciences and Technology of Oran Mohamed Boudiaf (USTO-MB),
El Mnaouer, PO Box 1505, Bir El Djir 31000, Oran, Algeria,
e-mail: abdelghani.belhanafi@univ-usto.dz, ladjedelomar@yahoo.com, adjlout@yahoo.fr

Manuscript received May 21, 2024; revised November 03, 2024

Abstract: The mixing of non-Newtonian fluids is a common phenomenon in industrial processes, where efficiency depends on the hydrodynamics of the stirring tank. A numerical study was conducted in a cylindrical vessel equipped with an agitator operating at a low Reynolds number. The liquid height was kept equal to the tank diameter. ANSYS CFD CFX was used to solve the numerical equations employing the MRF (Multiple Reference Frame) approach. The profiles and velocity distribution in vertical and horizontal planes were analyzed and discussed. The results show a reasonably good agreement with experimental data. To achieve a perfect circular flow in the vertical direction, the number of blades in the classical anchor was increased.

Keywords: Mixing, anchor agitator, blade number, laminar flow, CFD.

1. Introduction

Laminar mixing is commonly encountered in processes involving physical and chemical changes in many industries. The study of agitation systems has been initiated in several works. For example, Karray et al. [1] focused on the hydro-mechanical study of a cylindrical tank equipped with a classical anchor in a stationary regime. They examined the displacement effect of the anchor arm under turbulent flow conditions. Using CFD methods, Iranshahi et al. [2] compared the viscous mixing characteristics of the Ekato Paravisc mixer with those of an anchor and a double-helical ribbon. They found that the characteristics of the Paravisc mixer were between those of the other impellers at low Reynolds numbers. Zied et al. [3] proposed combining a classical anchor with the superposition of two turbine stages operating in a down-pumping direction to improve hydrodynamic flow. Ameur et al. [4] used a combination of Scaba 6SRGT and anchor agitators to enhance stirring efficiency for shear-thinning

liquids. Recently, Ameur et al. [5] tested newly designed impellers with a classical anchor in laminar regimes, resulting in improved fluid circulation and wider well-stirred regions for vessels equipped with circular horizontal blades.

Using CFD, Poonam and Farhad [6] focused on mixing xanthan gum, a pseudoplastic fluid with yield stress, using two-blade and four-blade anchor impellers. Their optimization study identified 0.102 and 0.079 as the optimal stirrer width-to-vessel diameter and stirrer clearance-to-vessel diameter ratios, respectively. They found that the anchor with four blades performed better than the two-blade version. Chhabra and Richardson [7] reported that anchors could be used for agitating both Newtonian and non-Newtonian fluids, primarily generating tangential flows with secondary axial and radial flows at high rotational speeds. Niedzielska et al. [8] experimentally investigated power consumption and heat transfer coefficients for ribbon impellers in laminar regimes. Nurul et al. [9] compared the torque produced by anchor and helical blade impellers for mixing highly viscous fluids (grease), finding that the helical blade produced 0.25 N·m, while the anchor blade produced 0.28 N·m. Anne-Archard et al. [10] used CFD to analyze hydrodynamics and power consumption in laminar flows, establishing Metzner-Otto correlations for power-law fluids and discussing shear rate distributions for helical and anchor agitators. Sinthuran et al. [11] studied gas dispersion in viscous Newtonian fluids using a coaxial mixer with a central impeller (PBT) and an anchor agitator, demonstrating its effectiveness in dispersing gas against buoyancy forces. Murthy et al. [12] developed a new correlation for calculating power consumption in anchor mixing systems using CFD simulations based on the Metzner-Otto concept. Abhishek et al. [13] proposed a novel method for measuring solid suspension in anchor-agitated vessels by observing density variations with different D/T ratios. Finally, Hae et al. [14] conducted experimental and numerical studies to examine unmixed regions in a tank equipped with an anchor impeller for Newtonian fluids.

The objective of this work is to study the mechanical agitation of a highly viscous fluid using an agitator in three configurations, based on increasing the number of blades in a tank equipped with an anchor impeller. This investigation aims to obtain the optimal impeller design for mixing viscoplastic fluids in a cylindrical tank, analyzed through CFD modeling.

2. Agitated systems

As presented in *Fig. 1*, three geometrically scaled vessels were chosen, each with a different number of blades on a classical anchor: an agitator with two blades (case 1), three blades (case 2), and four blades (case 3). The first system configuration is similar to the one described by Murthy et al. [12] (*Fig. 1*). Each system consists of a flat-bottom cylindrical vessel with a diameter of

$D = H = 0.3$ m. The anchor impeller has two arms with a diameter of $d = 0.9 \cdot D$ and a height of $h = 0.75 \cdot D$, attached to the shaft of the stirred vessel. The angle between the blades is $\theta = 180°$ for case 1, $\theta = 120°$ for case 2, and $\theta = 90°$ for case 3.

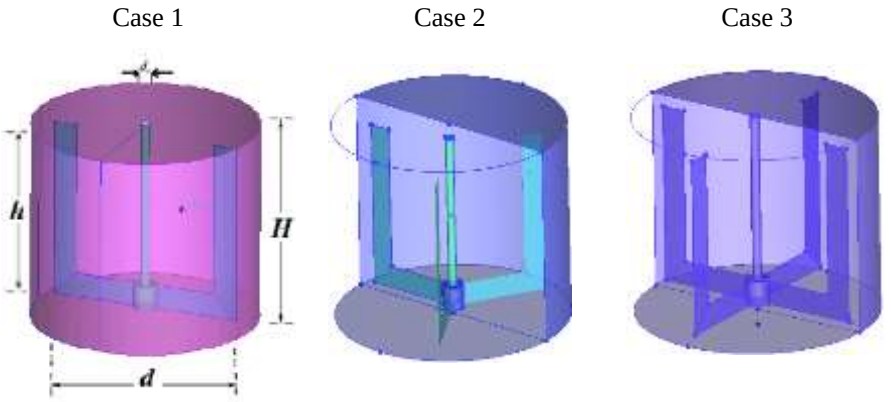

Figure 1: Mixing vessel dimensions

3. Method

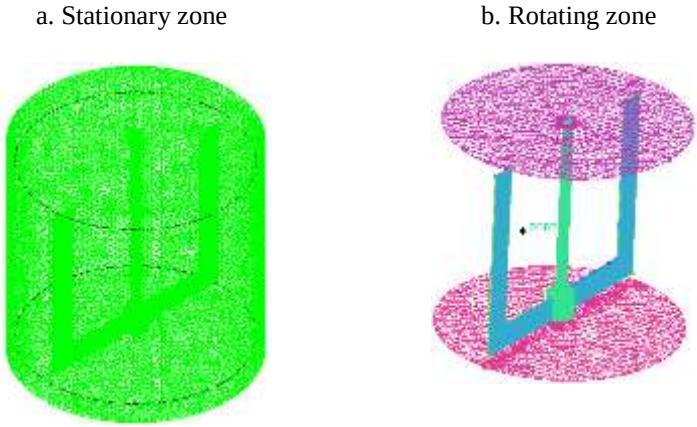

Figure 2: Tetrahedral mesh generation

Three-dimensional computational fluid dynamics (CFD) simulations were carried out using the CFD software ANSYS CFX to investigate the flow field in an agitated vessel stirred by a two-blade, three-blade, and four-blade anchor

agitator. The computational domain was meshed using tetrahedral cells in ANSYS ICEM CFD (*Fig. 2*). The domain was divided into two distinct zones for each of the three geometries. The tank walls constitute the stationary zone (*Fig. 2a*), discretized with 88,066 nodes. The rotating zone *(Fig. 2b*) describes the rotational motion of the fluid around the impeller and was discretized with 201,372 nodes for case 1, 276,234 nodes for case 2, and 341,948 nodes for case 3. Boundary conditions were defined in ANSYS CFX-Pre using the multiple reference frame (MRF) approach. In this approach, the interface between the two regions is treated by the frozen rotor method, which connects the flow fields at the interior surfaces (interface) separating the two domains. The computations were performed on a system with an Intel Core i7 CPU (2.20 GHz) and 8 GB of RAM.

4. Governing Equations

The Herschel-Bulkley model combines the effects of Bingham and power-law behavior in a fluid giving the shear stress as:

$$\tau = \tau_y + K \cdot \dot{\gamma}^n . \tag{1}$$

In (1), τ_y is the yield stress, K the consistency index, $\dot{\gamma}$ the shear rate and n is the flow behavior index. The average shear rate can be related to the impeller speed (N) by:

$$\dot{\gamma} = K_s \cdot N . \tag{2}$$

In (2), K_s is the Metzner-Otto's constant. The apparent viscosity results:

$$\eta = \frac{\tau}{K_s \cdot N} = \frac{\tau_y + K \cdot (K_s \cdot N)^n}{K_s \cdot N} . \tag{3}$$

The Reynolds number (Re) and the power number (N_p) are, respectively, calculated as:

$$Re = \frac{K_s \cdot N^2 \cdot d^2 \cdot \rho}{\tau_y + K \cdot (K_s \cdot N)^n} , \tag{4}$$

where d is the impeller diameter, and

$$N_P = \frac{P}{\rho \cdot N^3 \cdot d^5} . \tag{5}$$

In (5), ρ is the density of the fluid and P is the power consumption.

5. Results and discussion

5.1 Comparison with Experimental Results

Fig. 3 shows the radial profile of the dimensionless angular velocity component, defined for $\theta = 90°$. The comparison between the numerical results and the experimental results reported by Murthy et al. (2003) shows good agreement, demonstrating the validity of the adopted numerical method.

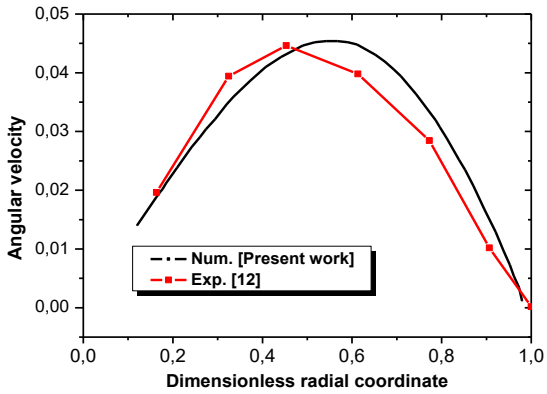

Figure 3: Radial profiles of the angular velocity at θ=90°

5.2 Effect of Blade number

5.2.1 Mean Velocity in r- θ Plane

a b c

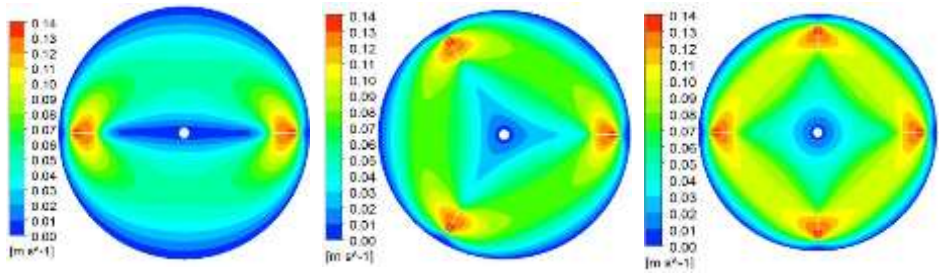

Figure 4: Mean velocity distribution in the horizontal plane:
$z = 0.15$ m, $N = 10$ rpm, $n = 0.8$

The results of the velocity contours at the mid-height of the tanks are illustrated in *Fig. 4*. Globally, it is noted that the maximum values of the wake are developed in the area swept by the blades in all three cases. In case 3, the recirculation loop is more extended throughout the entire volume of the tank, reducing the stagnant fluid zone (*Fig. 4c*). For the classical anchor agitator (*Fig. 4a*), the maximum values are concentrated around the two vertical arms. As clearly illustrated, increasing the number of blades enlarges the well-stirred region and ensures mixing throughout the entire vessel volume.

5.2.2 Velocity in r-z Plane

Fig. 5 represents the mean velocity distribution in three different vertical planes for the tank. In this figure, the blue regions indicate stagnant (unmixed) zones, while the red regions indicate areas of high mixing caused by the impeller. Comparing these configurations, it is noted that the velocity is very low in the classical anchor configuration, case 1 (*Fig. 5a*). In the two other configurations, case 2 and case 3 (*Fig. 5b* and *Fig. 5c*), the maximum values of the mean velocity appear near the mechanical source and begin to decay continuously until becoming negligible near the shaft. In contrast, no recirculation motion is observed at the center of the stirred vessel in case 1 (*Fig. 5a*). Indeed, the anchor with three blades creates larger circulation loops of mean velocity between the blades in case 2 (*Fig. 5b*).

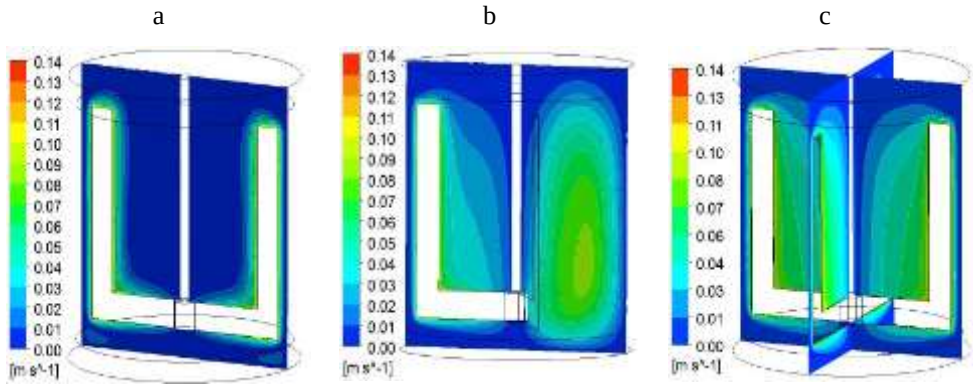

Figure 5: Mean velocity distribution in the vertical plane: N = 10 rpm, n = 0.8

On the horizontal plane, the mean velocity distribution is shown at the top parts of the vessels. In each case, a low-velocity region was observed behind the vertical arm, likely due to the contact surface between the blades and the fluid. In the first system, large non-agitated zones are observed (*Fig. 6a*). These dead zones can be reduced or eliminated by increasing the number of blades.

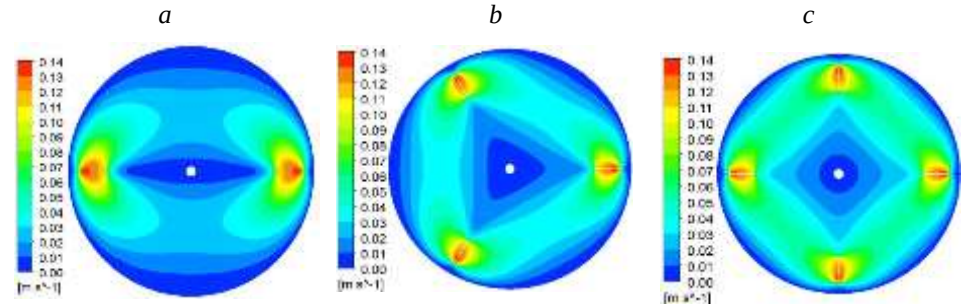

Figure 6: Mean velocity distribution in the horizontal plane, on the top, N = 10 rpm, n = 0.8

5.2.3 Streamlines

A 3D configuration of streamlines is shown in *Fig. 7*. This figure illustrates a highly turbulent mixing flow, particularly at the central parts of the vessels for the 2nd and 3rd configurations (*Fig. 7b* and *Fig. 7c*). Unlike the two-blade anchor in case 1, a small single loop of streamlines is observed at the mid-height of the tank (*Fig. 7a*). The primary circulation loop of streamlines is observed at the vessel base for the four-blade anchor agitator (*Fig. 7c*). This suggests that this type of impeller distributes the fluid more evenly throughout the volume. The three-blade anchor agitator directs the fluid toward the free surface of the liquid (*Fig. 7b*). This phenomenon was not observed in the classical anchor configuration, case 1 (*Fig. 7a*).

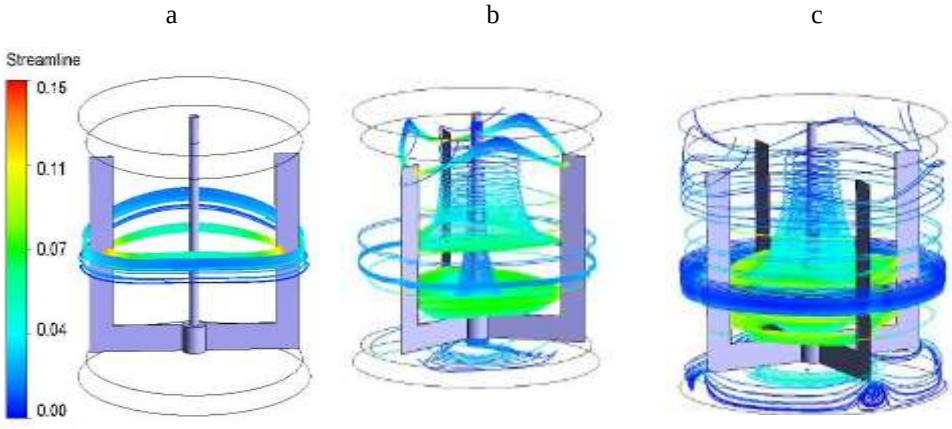

Figure 7: Streamlines for three cases: N = 10 rpm, n = 0.8

5.2.4 Dimensionless velocity profiles

5.2.4.1 Radial velocity component

The profiles shown in *Fig. 8* represent the distribution of dimensionless radial velocity for the three cases. From the velocity components, it can be seen that the fluid is well distributed in the radial direction. At R = 0.075 m, the distribution of radial velocity increases with the increasing number of blades. This is due to the effect of the number of arm contact surfaces on the fluid dynamics. The radial component is more significant for the two configurations: case 2 and case 3. However, in the tank equipped with the classical anchor (case 1), the velocity is very low. Arguably, the radial velocity component is affected by the number of blades.

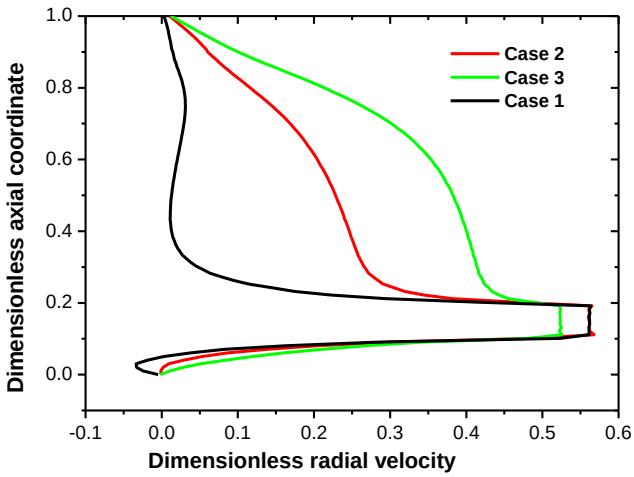

Figure 8: Radial velocity at radial position R = 0.075 m, N = 10 rpm, n = 0.8, θ = 30°

5.2.4.2 Tangential Velocity component

The tangential velocity along the tank radius is plotted in *Fig. 9* for a rotational speed of N = 10 rpm. As observed in configuration case 3, the tangential velocity increases gradually until reaching the highest values at the blade tip, then decreases rapidly at the vessel wall. This dynamic phenomenon is due to the acceleration of the fluid resulting from the increased number of blades on the agitator. However, in the first case, the velocity is very low compared to the other configurations, due to the large space between the two vertical arms of the classical anchor. The optimum values are obtained for tanks equipped with three and four blades, with V^* = 0.33 at R^* = 0.98.

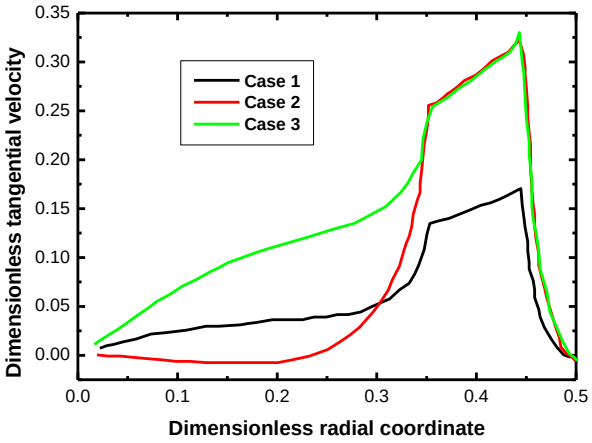

Figure 9: Tangential velocity at axial position z = 0.150 m, N = 10 rpm, n = 0.8, θ = 45°

6. Conclusion

The objective of this work was to determine the effect of different impeller types of anchor agitators in a cylindrical tank. From the presented results, the following conclusions can be drawn.

The anchor with three blades (case 2) creates larger amplitude circulation loops of mean velocity between the vertical arms. A high turbulence behavior of the streamlines is observed in the central part of the tanks for case 2 and case 3. In contrast to the classical anchor (case 1), a small single loop of streamlines is observed at mid-height of the tank. This is due to the large space between the two vertical arms of the classical anchor. It has been clearly observed that the dimensionless velocities in the radial direction are directly affected by the number of blades.

It can be concluded that when the number of arms is increased from 2 to 4, the flow is directly affected by the new active mixing region throughout the entire volume of the tank.

References

[1] Karray, S., Driss, Z., Kchaou, H., Abid, M. S., "Numerical simulation of fluid-structure interaction in a stirred vessel equipped with an anchor impeller", *Journal of Mechanical Science and Technology*, vol. 25 (7), pp. 1749–1760, 2011.

[2] Iranshahi, A., Heniche, M., Bertrand, F., and Tanguy, P. A., "Numerical investigation of the mixing efficiency of the Ekato Paravisc impeller", *Chem. Eng. Sci*, vol. 61, pp. 2609–2617, 2006.

[3] Archard, A., Marouche, M., and Boisson, H. C., "Hydrodynamics and Metzner-Otto correlation in stirred vessels for yield stress fluids", *Chem. Eng. J*, vol. 125, pp. 15–24, 2006.
[4] Ameur, H., and Ghenaim, A., "Mixing of Complex Fluids in a Cylindrical Tank by a Modified Anchor Impeller", *Energy Technology & Environmental Science*, vol. 3, pp. 7472–7477, 2018.
[5] Ameur, H., and Youcefi, S., "Newly suggested shapes of impellers for stirring highly viscous fluids in vessels", *Science paper*, vol. 35, pp, 1–20, 2021.
[6] Prajapati, P., and Mozaffari, F.E., "CFD Investigation of the Mixing of Yield-Pseudoplastic Fluids with Anchor Impellers", *Chem. Eng. Technol*., vol. 32 (8), pp. 1211–1218, 2009.
[7] Chhabra, R.P., and Richardson, J.F., "Non-Newtonian flow in the process industries", Fundamentals and engineering applications, Butterworth-Heinemann, 1999.
[8] Niedzielska, A., and Kuncewicz, C., "Heat transfer and power consumption for ribbon impellers", *Mixing efficiency Chemical Engineering Science*, vol. 60, pp. 2439–2448, 2005.
[9] Nurul, F. M. Y., Edmund, U. E., Ismail, F. I., and Akmal, N. M., "Mixing Performance of Anchor and Helical Stirrer Blades for Viscous Fluid Applications", *CFD Letters*, vol. 13.1, pp. 58–71, 2021.
[10] Driss, Z., Salah, A. D., Driss, B., Necib, H., Kchaou, B., and Abid, M.S., "CFD investigation of the hydrodynamic structure around a modified anchor system", in *CFD Techniques and Energy Applications*, pp. 129–150, 2018.
[11] Sinthuran, J. Argang, K. A., and Farhad, E.-M., "Enhanced aeration efficiency in non-Newtonian fluids using coaxial mixers: High-solidity ratio central impeller with an anchor", *Chemical engineering Journal*, 378, pp. 122081. 2019.
[12] Murthy, S., and Jayanti, K., "Mixing of Power-Law Fluids Using Anchors: Metzner-Otto Concept Revisited", *AIChE Journal, January*, vol. 49, pp, 30–40, 2003.
[13] Abhishek, M. S., Choudhari, S., and Muller. F., "Observations of solid–liquid systems in anchor agitated vessels", *Chemical engineering research and design*, vol. 90, pp. 750–756, 2012.
[14] Hae, J. J., Hye, K. J., Young, J. K., and Wook, H. R., "Analysis of dynamical systems structures and mixing patterns in an anchor agitator", *Journal of chemical engineering of Japan*, vol. 51, no. 2, pp, 136–142, 2018.
[15] Belhanafi, A., Driss, Z., and Abid, M. S., "Pumping Effects of a Square Tank Equipped with Single-Stage and Bi-Stage Impellers", *Acta Universitatis Sapientiae Electrical and Mechanical Engineering*, vol. 14, pp. 1–12, 2022.
[16] Belhanafi, A., and Touhami, B., "Numerical study of bottom shape effect on the mixing for stirred tank", *Acta Universitatis Sapientiae Electrical and Mechanical Engineering*, vol. 15, pp. 86–97, 2023.